RSMC Tokyo – Typhoon Center

Technical Review

No. 6

Contents

Japan Meteorological Agency

March 2003

The Development of Guidance for Forecast of Maximum Precipitation Amount

Satoshi Ebihara
Numerical Prediction Division, JMA

1. Introduction

Since 1980, the Japan Meteorological Agency (JMA) has developed various forecast guidance products based on statistics of numerical prediction output to assist operational forecasting. From the disaster mitigation point of view, emphasis is placed particularly on the guidance for precipitation such as Maximum Precipitation Guidance (MaxP) and Area-mean Precipitation Guidance (MeanP), which provide forecasts of respective maximum and area-mean precipitation for 1-, 3- and 24- hour periods for each of about 300 forecast zones designated for information services. The first version of MaxP (hereinafter, the old MaxP) was developed in July 1996 and used until May 2002. In June 2002, JMA developed and put into operation the second version of MaxP (hereinafter, the new MaxP) which was improved especially eliminating the strong bias inherent in the old MaxP toward less frequency in prediction of heavy precipitations.

In this paper, an outline of the old MaxP is first presented together with several problems involved in the guidance. Secondly, the process of developing the new MaxP is described and its performance is compared with that of the old MaxP. Finally, an example of forecasts made by the new MaxP for the heavy rainfall associated with a tropical cyclone is shown.

2. Outline of the old MaxP

Main features of the old MaxP were as follows:

i) Prediction was made with a 3-hour precipitation amount for each of the 0.4° (lat.)×0.5° (lon.) (≒40 km×40 km at 35° N) meshes in the forecast domain covering the Japanese islands.
ii) The Neural Network (NRN) was used to derive MaxP for the meshes (a brief description of NRN is given in Appendix I).
iii) A MaxP for a forecast zone ranging over more than one mesh was defined as the maximum of the MaxPs for the relevant meshes.
iv) Analyses of maximum precipitations to be used for deriving

predictand data of NRN were prepared from radar precipitations calibrated with rain gauge observations (Radar-AMeDAS Precipitation Analyses, hereinafter Radar-AMeDASs; see Appendix II).

v) The Regional Spectral Model (RSM) of JMA provided the values of several input data predictors for NRN.

During the six years of its operational use, the following problems were identified in the old MaxP:

a) Predictions are much less frequent than actual for heavy precipitations (e.g. ≧ 30mm/3h), while more frequent for light precipitations (e.g. ≦5mm/3h).
b) Many of the forecast zones were smaller than the mesh size and, accordingly, MaxP could not be well representative.
c) The 24-hour MaxPs tended to be overestimated because they are calculated by simply integrating 3-hour MaxPs.

3. A scheme adopted to develop the new MaxP

In order to solve the problems as described above, the following scheme was adopted for the operational procedures to produce the new MaxP;

I) Max-Mean Precipitation Ratio (MMPR; defined as maximum/mean precipitation) is calculated in the first place.
II) MaxP are calculated by multiplying MeanP with MMPR.

MeanP is calculated by the Kalman filter for each of the 0.2° (lat.)×0.25° (lon.) (≒20 km×20 km at 35° N) mesh. It should be noted that MeanP does not have a bias toward less frequent prediction of heavy precipitations (the Kalman filter and the calculation process for MeanP is given in the Appendix III). A MeanP for a forecast zone is obtained by averaging MeanPs for the relevant meshes in the zone. MMPR for a forecast zone is calculated by NRN with prognostic outputs of the Regional Spectral Model (RSM) and a MeanP listed below as input data:

(a) Wind direction at 850 hPa
(b) Wind speed at 850 hPa
(c) Showalter Stability Index (SSI)
(d) Difference between 1000-hPa specific humidity and 400-hPa saturated specific humidity
(e) Thickness of moist layer

(f) Index of orographic precipitation
(g) MeanP

Weights of NRN were adjusted through the learning process with archived data for the four years from 1997 to 2000, including mean and maximum precipitations derived from the Radar-AMeDASs at a 5 km resolution. In the calculation of MMPR in operation, NRN runs with fixed weights. On this account, RSM outputs, of which characteristics are highly susceptible to model modifications, such as vertical velocities in pressure and precipitation amounts, were not adopted as input data. Accordingly, if MMPRs are realistic, the problem of less frequency in prediction of heavy precipitation will be not occur;

→ the problem a) will be cleared.

Further, since the resolution of the precipitation analysis is finer (5km× 5km), MMPR is expected to well represent the locality at any forecast zone and so is MaxP as a result;

→ the problem b) will be solved.

The problem c) will be also negligible because 1-, 3- and 24-hour MaxPs are estimated independently.

4. Characteristics of MMPR and the new MaxP

Characteristics of MMPR and the new MaxP were examined by use of observations (Radar-AMeDASs) and the result for a forecast zone in Shizuoka Prefecture for the period from April 2001 through March 2002 are presented in Figure 1.

On the top are the figures showing comparisons of MMPRs between observations and estimations which were calculated by use of mean precipitations (observations) in place of MeanPs. These figures indicate that the estimated MMPRs present the same feature as shown by observational MMPRs, thus suggesting that MMPR is realistic.

The figures at the middle show the maximum possible performance of the new MaxP; MaxPs were obtained with mean precipitation (observations) in place of MeanPs. The distributions of the MaxPs relative to the observations in the figures show no significant bias in the MaxP performance such as less frequencies in heavy precipitation predictions.

Actual performance of the new MaxP in this case is presented in the figures at the bottom; MaxPs were calculated through the operational procedures using MeanP. It should be noted that the almost evenly distributed MaxPs relative to observations similarly as above figures suggests the reasonableness of the new guidance.

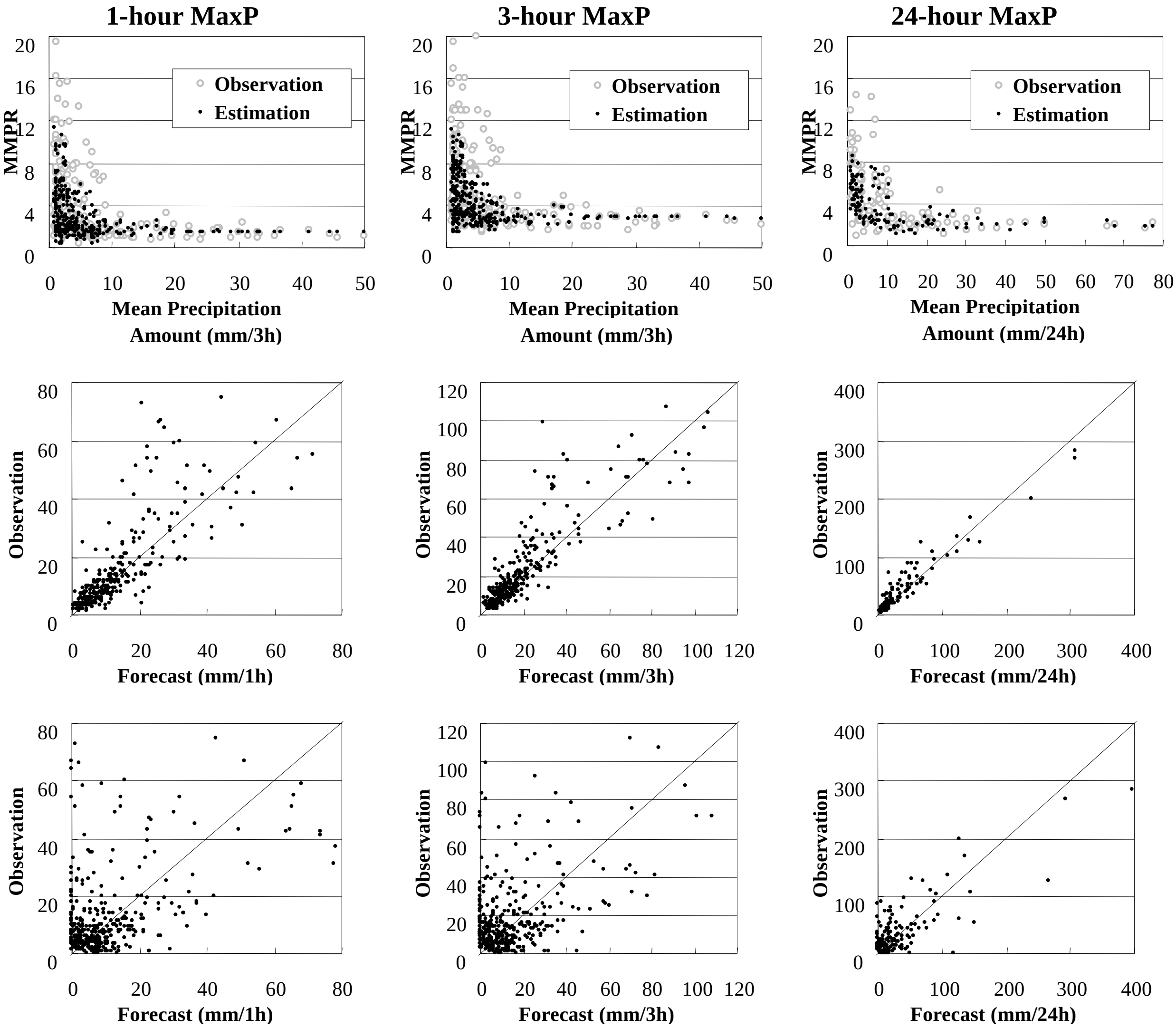

Fig. 1 Characteristics of MMPRs and the new MaxP for 1-, 3- and, 24-hour predictions in the central Shizuoka Prefecture. The data were taken from a period independent of the period for NRN learning.

5. Comparison of performance between the new and old MaxPs

Figure 2 presents bias and threat scores of the new and old MaxPs for 3-hour precipitations, which were calculated using the data for April through September 2001. As shown in the Figure, the large biases demonstrated by the old MaxP were significantly improved by the new MaxP. Differences are particularly noticeable in both bias and threat scores for the forecasts of light rains (5mm/3h) and heavy rains (30mm/3h).

Deterioration of the bias and threat scores of the new MaxP for the forecast times of 18 hours and longer is attributed to the afternoon showers which occur during the forecast hours in the warm season and are too small in scale for MeanP to accurately predict. The locality of those convective precipitations also boosts the values of observational MMPR, which leads to degradation of MMPR estimations and thus worsens the scores.

Figure 3 is the same as Figure 2 but for the new MaxP for 1-hour precipitations. As shown in the Figure, basic features are common between the two Figures including reasonable performances for heavy precipitations except for the forecast hours of afternoon showers.

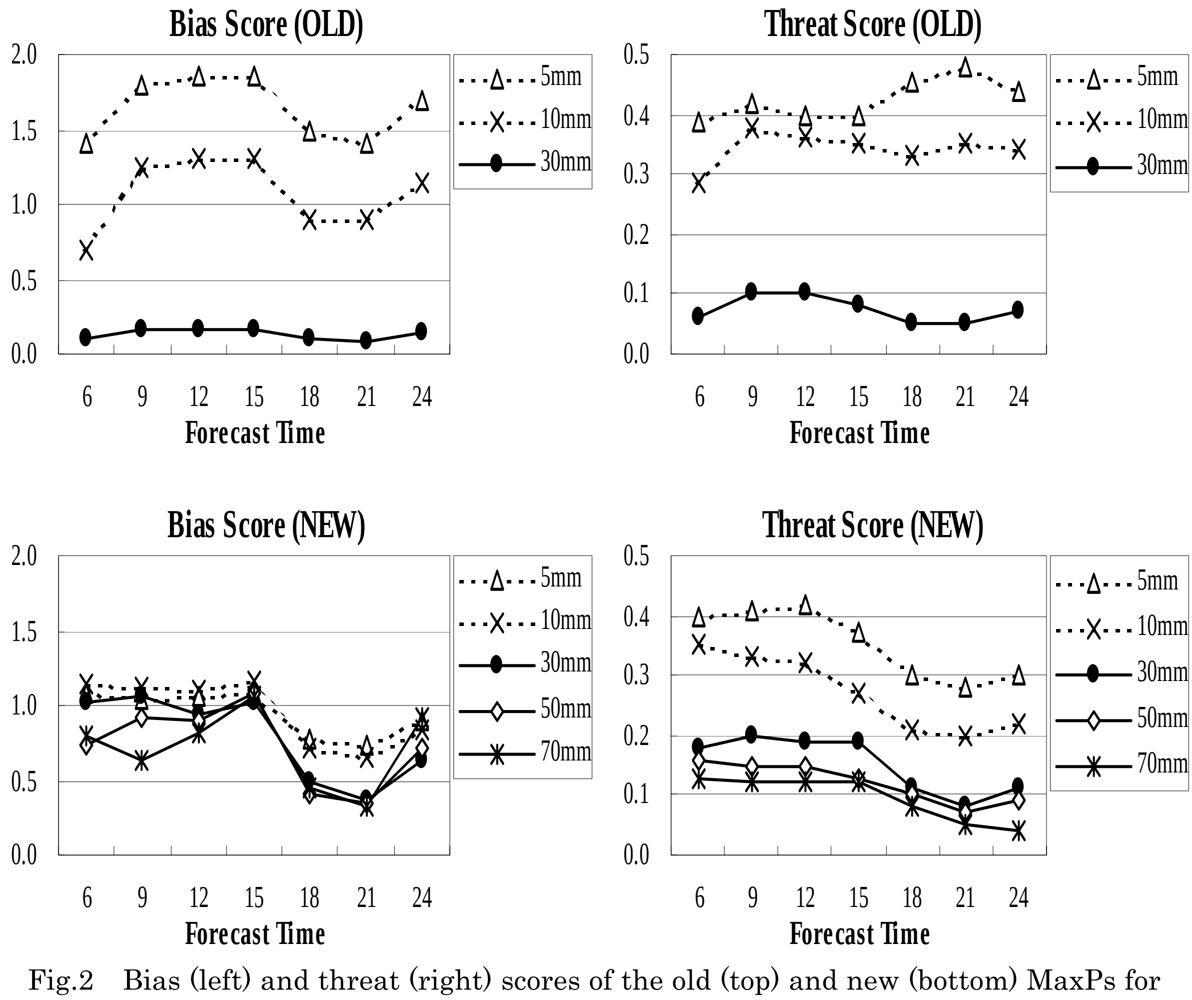

Fig.2 Bias (left) and threat (right) scores of the old (top) and new (bottom) MaxPs for 3-hour precipitation; initial time for NWP is 12UTC, and predictions at t+03h (00LST) - t+24h(21LST) were verified.

Figure 4 shows the threat and bias scores of the new and old MaxPs with respect to precipitation intensities (mm/24hours). The old MaxP has large bias scores of around 2.0 for intensities of less than 100mm/24h, while small bias scores of around 0.5 for the high intensity of 200mm/24h (heavy precipitation) .
The new MaxP shows no significant biases even for heavy precipitations and has improved threat scores for the almost full range of precipitation intensities by roughly 0.1 as compared to the old MaxP

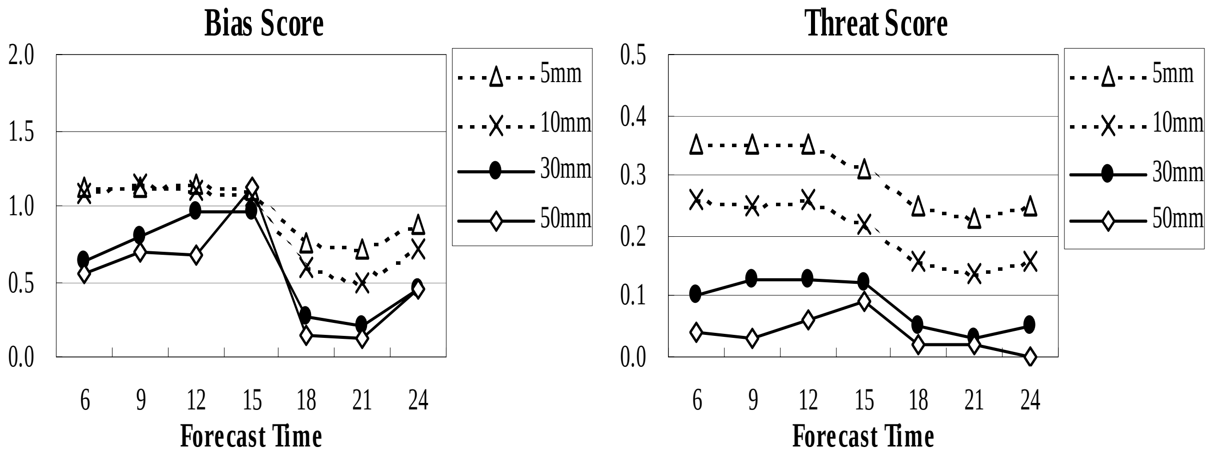

Fig.3 Bias and threat scores of the new MaxP for 1-hour prediction.

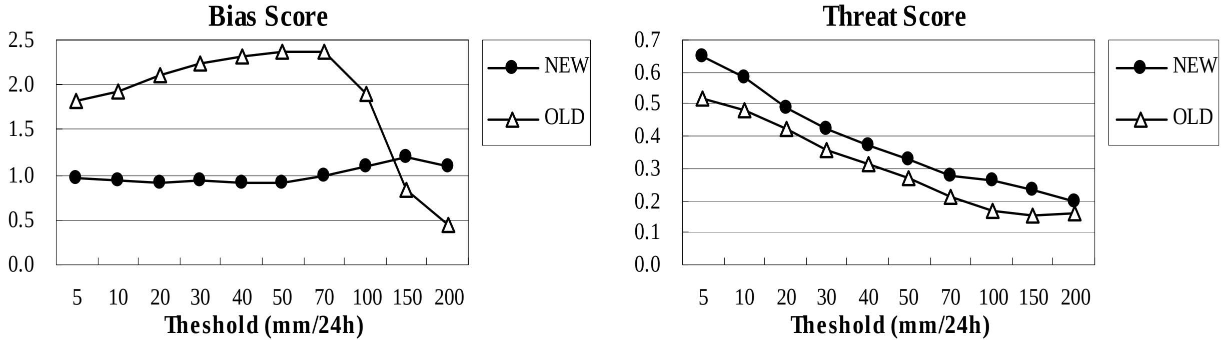

Fig.4 Bias and threat scores of the old and new MaxPs for 24-hour prediction for the period from April to September 2001.

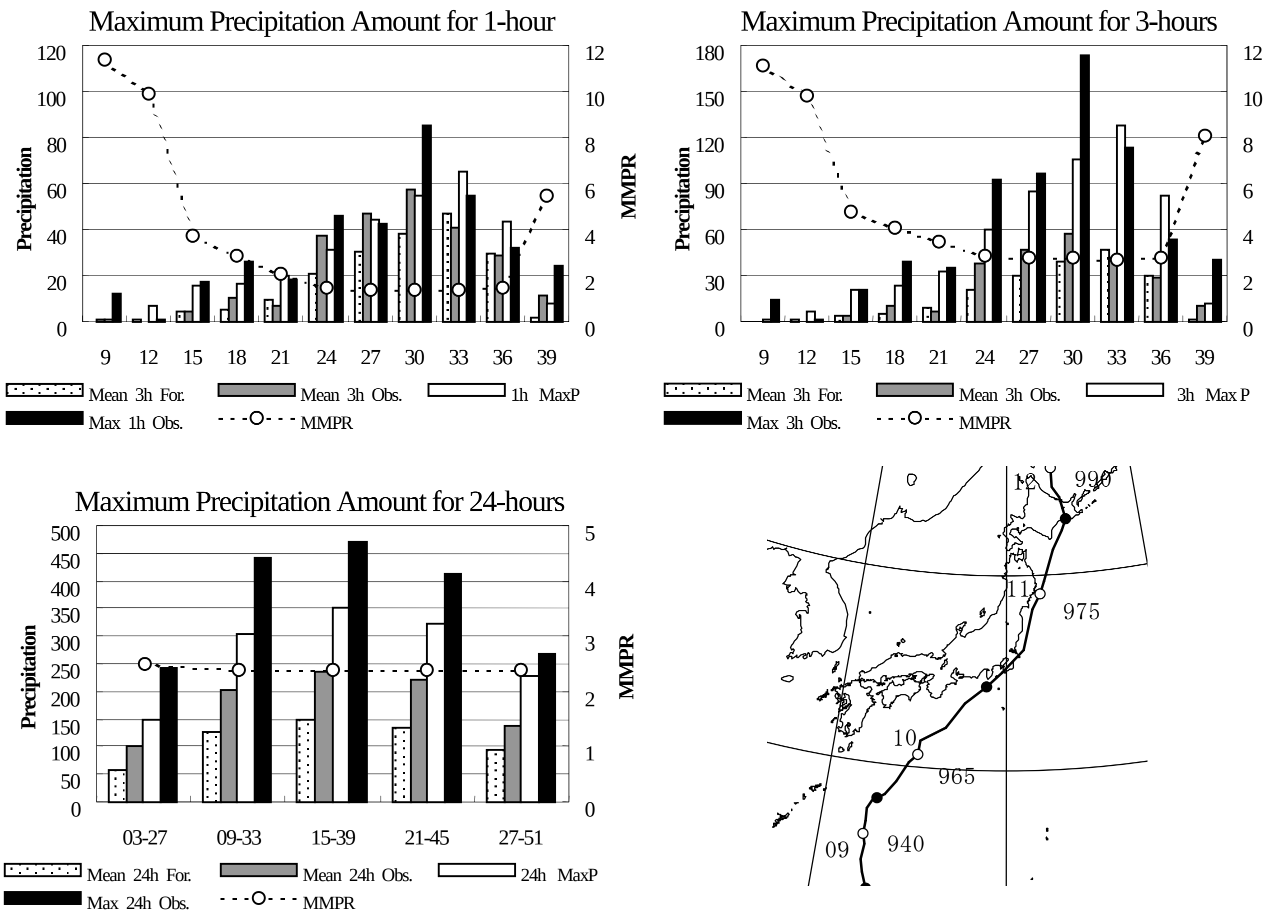

Best Track Typhoon Chataan (0206)

Fig.5 Performance of the new MaxP in the central Shizuoka Prefecture when Typhoon Chataan(0206) was approaching Japan. The initial time of the prediction was 00UTC 9 July 2002.

6. An example of performance of the new MaxP

Figure 5 shows predictions of the new MaxP in comparison to analyses (Radar-AMeDAS) in the case of a heavy rain in the central Shizuoka Prefecture in July 2002. The rain was produced by the interaction of a stationary front with Typhoon Chataan (0206) which was approaching Japan. As indicated in the Figure, 1- and 3-hour MaxPs with initial time of 00 UTC July 9 adequately predicted the peak of the rain as well as heavy showers of 50mm/1h and 100mm/3h which requires alarming in this forecast zones. Although 24-hour MaxP consistently fell short of observations due to the underestimation of MeanP, it did not miss the critical hours (t=09-33) when 24-hour precipitation reached the warning criteria of 250mm/24h.

7. Summary

MaxP, a forecast guidance product for the maximum precipitation, was upgraded and became operational in June 2002. The new version of MaxP is calculated from MMPR (maximum/mean precipitation ratio) and MeanP (mean precipitation), which are derived by the Neural Network and the Kalman filter, respectively. Biases were notably eliminated in the new MaxP, particularly those of “less frequency in prediction of heavy precipitations” and “excessive frequency in prediction of light precipitations”. The finer resolution of MMPR allowed MaxP to be well representative even in the small forecast zones. However, upgrade of MeanP has been also encouraged due to its considerable impact on the performance of MaxP.

Appendix Ⅰ, Ⅱ, Ⅲ are quotations from "OUTLINE OF THE OPERATIONAL NUMERICAL WEATHER PREDICTION AT THE JAPAN METEOROLOGICAL AGENCY" March 2002.

Appendix I

(a) Neural Network

The Neural Network (NRN) is one of the Artificial Intelligence methods and is an effective technique to analyze non-linear phenomena. Its basic element is called a "neuron", and multiple neurons are linked together to construct a hierarchical neural network, as shown in Fig. I -4. The first layer is called the "input layer", the last layer is called the "output layer", and the layers between them are called "hidden layers".

When a signal is put into the input layer, it is propagated to the next layer through the interconnections between the neurons. Simple processing is performed on this signal by the neurons of the receiving layer prior to its being propagated on to the next layer. This process is repeated until the signal reaches the output layer.

A schematic diagram of a neuron is shown in Fig. I -1. The input of each neuron is a weighted sum of the outputs of other neurons, and the output is a function of its input. This function is called an "activation function", and a sigmoid function shown in Fig. I - 2 is usually used.

The weights of NRN are iteratively adjusted through learning numerous sets of input/output data. The most popular way to adjust weights is the "back propagation of error" algorithm described as follows:

(i) At first, weights are initialized with randomized values.

(ii) The NRN gets a set of input values and calculates output.

(iii) The weights are adjusted to make the NRN output approach the "supervisor data" (correct values of the output variable).

(iv) Processes of (ii) and (iii) are iterated until the error measure falls below a specified value or a specified maximum number of iterations is reached.

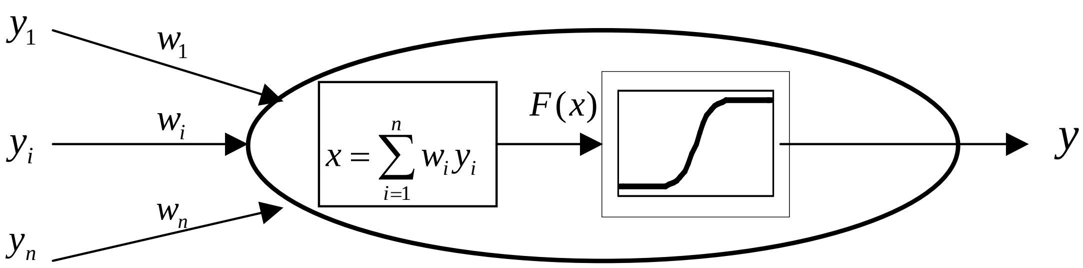

Fig. I -1 A schematic diagram of a neuron.

$$F(x) = \frac{1}{1+e^{-(2/c)x}}$$

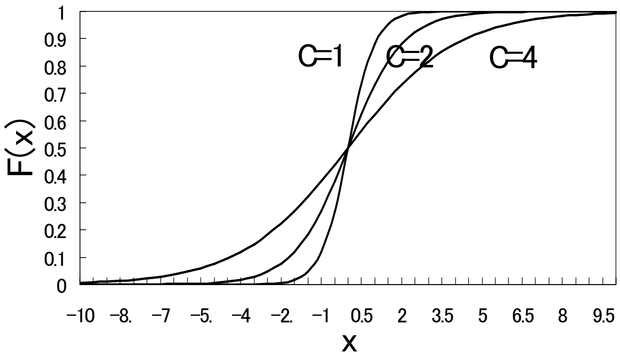

Fig. Ⅰ-2 Examples of sigmoid function.

(b) An example of the guidance by Neural Network (Categorized weather)

In the forecast guidance system, a Neural Network model is constructed at each grid or observation point from the sets of NWP output and observed weather elements. Categorized weather is one of the forecast guidance parameters to which NRN is applied. Fig. Ⅰ-3 shows an output example of categorized weather guidance. In this guidance, a NRN model is used to derive sunshine duration, which is used to determine the non-precipitating weather categories (fair or cloudy). The NRN is constructed at each AMeDAS station, and output values (3-hourly sunshine duration) are interpolated to grid points. The precipitating weather categories (rainy, sleety, snowy) are determined from the KF-based precipitation amount guidance. The constitution of the sunshine duration NRN model is shown in Fig. Ⅰ-4, and its characteristics are summarized as follows:

(i) It is a 3-layered Back Propagation Network.
(ii) As an activation function of each neuron, a linear function is used in the input and output layer, and a sigmoid function is used in the hidden layer.
(iii) In learning processes, NWP output is used as input data, and sunshine duration observed at each AMeDAS point is used as supervisor data.
(iv) The weights of the network are modified at every time when the observation corresponding to the forecast is obtained.

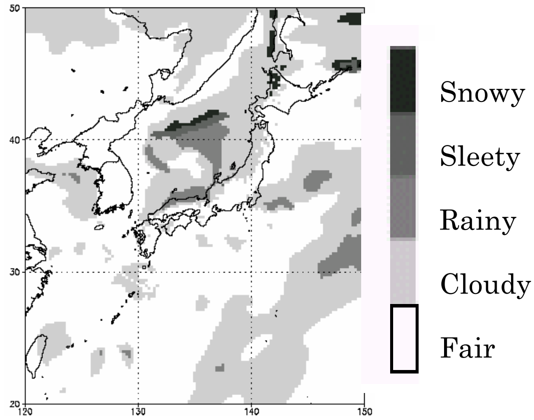

Fig.　I -3　An example of output of the categorized weather guidance

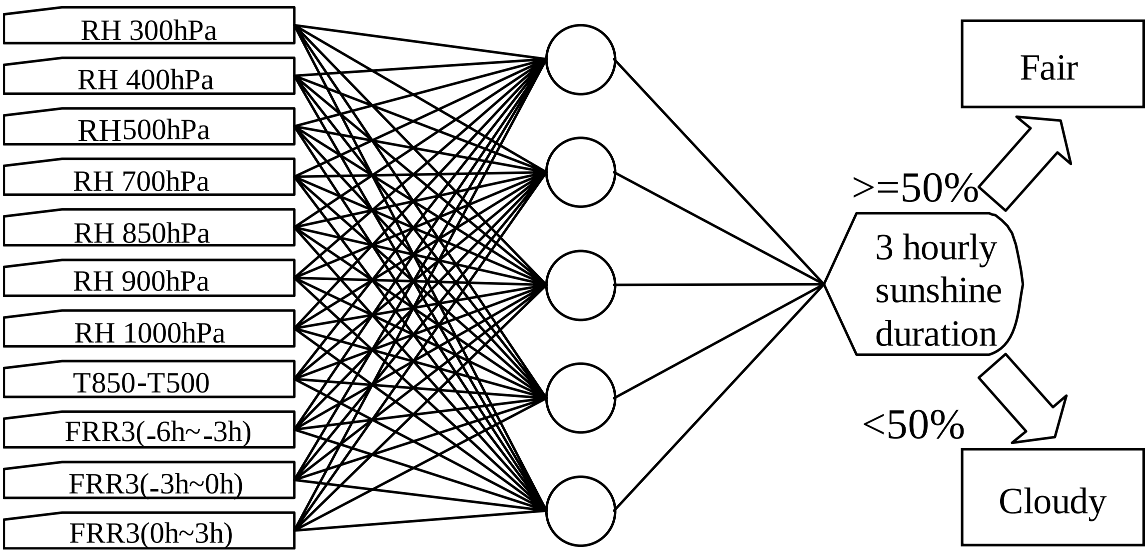

Fig.　I -4　Neural Network for fair / cloudy determination.
RH: Relative humidity,　FRR3: Precipitation over 3 hours

Appendix Ⅱ

Analysis of precipitation

Twenty conventional radars and the AMeDAS, which consists of a network of approximately 1300 automatic raingauge stations, provide observational data for the Radar-AMeDAS precipitation analysis. The data are combined to benefit from the advantages of both facilities: the advantage of the radar is its high resolution in space and that of AMeDAS is its accuracy of precipitation measurement with an average spacing of nearly one station per 17km by 17km.

On each radar site, the power scattered from rain particles is received and digitized by an automatic data processing system called “Radar Echo Digitizing and disseminating System (REDIS)”. Ground clutter is automatically removed through a Moving Target Indicator (MTI) filter by REDIS. A Z-R relationship is used for the conversion from the radar reflectivity factor to rainfall intensity. The horizontal resolution of the intensity data is 2.5km at the lowest altitude, and 5km at the other altitudes. One-hour accumulated radar precipitation amounts are calculated from the rainfall intensities.

The one-hour accumulated radar precipitation amounts are usually different from those observed with the AMeDAS raingauges. The radar precipitation amounts are calibrated with the AMeDAS precipitation data into more accurate precipitation. First, calibration factors over the entire detection range of each radar are calculated by comparing the radar precipitation of the multiple radars and raingauge data. When comparing radar precipitation, the difference of radar beam height is taken into account. Then the estimated calibration factor is modified at each grid over land using raingauge data. For the grid within which no AMeDAS raingauges are contained, the calibration factors are interpolated from those with AMeDAS raingauges. Composition of each radar’s calibrated precipitation into a nationwide chart is made by the maximum method, in which the largest radar precipitation among the several different radar observations on the same grid is selected. A schematic diagram of this procedure is shown in Figure Ⅱ-1.

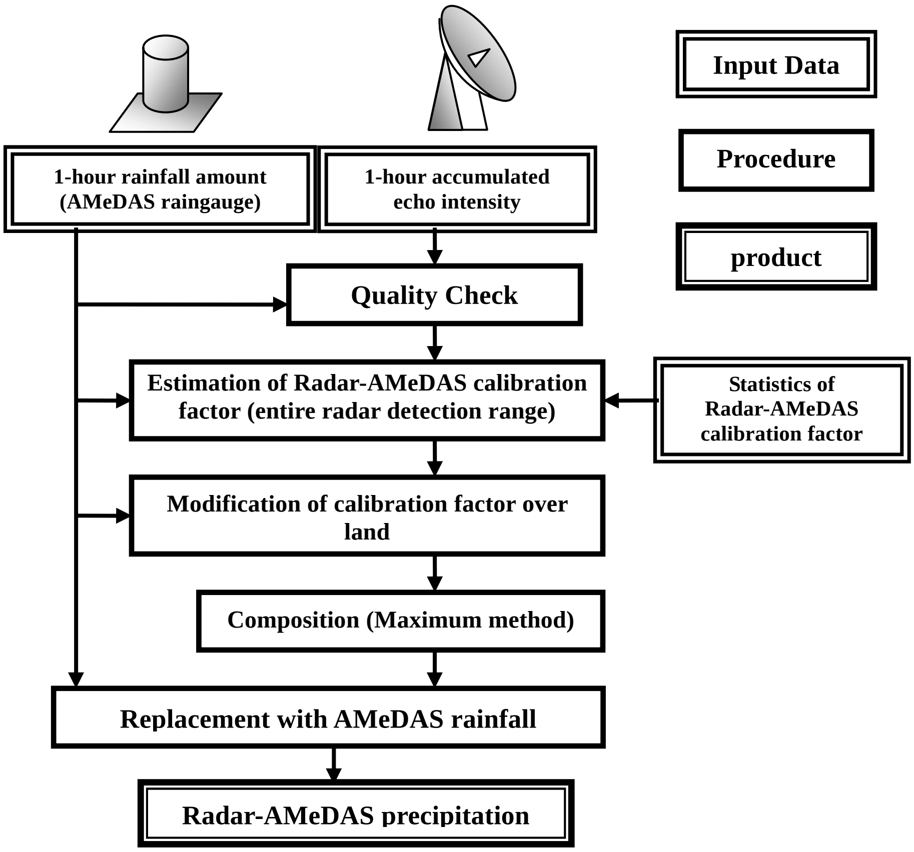

Figure Ⅱ-1 A schematic diagram of the “Radar-AMeDAS precipitation” analysis

Appendix Ⅲ

Guidance by Kalman Filter

(a) Kalman Filter

Kalman Filter (KF) as a statistical post-processing method of NWP output was developed in JMA on the basis of earlier works of Persson(1991) and Simonsen(1991). The notation of KF, which basically follows that of Persson(1991), is as follows:

y : predictand (target of forecast)
$\boldsymbol{c}$: predictors (1 × n matrix)
$\boldsymbol{X}$: coefficients (n × 1 matrix)
$\boldsymbol{Q}$: covariance of $\boldsymbol{X}$ (n × n matrix)
τ : sequence number of NWP initial times

First, the observation equation, which is a linear model for relating the predictand with pre-selected predictors, and the system equation are given as:

$$y_\tau = \boldsymbol{c}_\tau \boldsymbol{X}_\tau + v_\tau \tag{Ⅲ-1}$$
$$\boldsymbol{X}_{\tau+1} = \boldsymbol{A}_\tau \boldsymbol{X}_\tau + \boldsymbol{u}_\tau \tag{Ⅲ-2}$$

where v_τ is the observational random error whose variance is D_τ, and $\boldsymbol{u}_\tau$ is the random error vector of the system whose covariance matrix is $\boldsymbol{U}_\tau$. The matrix $\boldsymbol{A}_\tau$ describes the evolution of the coefficients in time and is set to the unit matrix in this case;

$$\boldsymbol{A}_\tau \equiv \boldsymbol{I} \tag{Ⅲ-3}$$

The objective of KF is to obtain the most likely estimation of the coefficients $\boldsymbol{X}_{\tau+1/\tau}$, whose subscripts denotes that this is estimated using the observation corresponding to the forecast at τ and used for the prediction at $\tau+1$. In contrast, single subscripts in eqs.(Ⅲ-1, 2) denote the “true” values at τ. $\boldsymbol{X}_{\tau+1/\tau}$ is obtained from the previous estimate $\boldsymbol{X}_{\tau/\tau-1}$ and the forecast error:

$$\boldsymbol{X}_{\tau+1/\tau} = \boldsymbol{X}_{\tau/\tau} \tag{Ⅲ-4}$$
$$= \boldsymbol{X}_{\tau/\tau-1} + \delta_\tau (y_\tau - \boldsymbol{c}_\tau \boldsymbol{X}_{\tau/\tau-1}) \tag{Ⅲ-5}$$

where

$$\delta_\tau = \boldsymbol{Q}_{\tau/\tau-1} \boldsymbol{c}_\tau^{\mathrm{T}} (\boldsymbol{c}_\tau \boldsymbol{Q}_{\tau/\tau-1} \boldsymbol{c}_\tau^{\mathrm{T}} + D_\tau)^{-1} \tag{Ⅲ-6}$$

$\boldsymbol{Q}$, the covariance of $\boldsymbol{X}$, is updated as follows:

$$\boldsymbol{Q}_{\tau+1/\tau} = \boldsymbol{Q}_{\tau/\tau} + \boldsymbol{U}_{\tau} \qquad (\text{III-7})$$
$$= \boldsymbol{Q}_{\tau/\tau-1} - \delta_{\tau}\boldsymbol{c}_{\tau} \quad \boldsymbol{Q}_{\tau/\tau-1} + \quad \boldsymbol{U}_{\tau} \qquad (\text{III-8})$$

Eqs. (Ⅲ-4) and (Ⅲ-7) are derived from (Ⅲ-2)-(Ⅲ-3).

Finally, the forecast value is calculated with the updated coefficients and predictors at $\tau+1$;

$$y_{\tau+1/\tau} = \boldsymbol{c}_{\tau+1}\boldsymbol{X}_{\tau+1/\tau} \qquad (\text{III-9})$$

For some forecast parameters, temperature for example, the predictand y is the difference between the NWP output and the observation, while for the others, precipitation amount for example, y is the observation itself. In the case of wind, u and v components are treated simultaneously with the predictand y as a complex number.

In the forecast guidance system with KF, D_{τ} and $\boldsymbol{U}_{\tau}$ in eqs.(Ⅲ-6) and (Ⅲ-8), respectively, are treated as empirical parameters of controlling the adaptation speed.

(b) Frequency bias correction

With KF, the most likely estimation of the predictand which minimizes the expected root-mean-square error is obtained. However, the output has a tendency of lower frequency of forecasting rare events, such as strong wind or heavy rain, than the actual. To compensate this unfavorable feature, a frequency bias correction scheme is applied to the KF output of some parameters.

The basic idea is to multiply the estimation of KF, y, by a correction factor $F(y)$ to get the final output y^b :

$$y^b = y \cdot F(y)$$

To determine $F(y)$, a number of thresholds t^i are fixed so that the forecast frequency over them should be approximating to that of observation. The objective of the scheme, then, is to find f^i corresponding to each t^i that determines the correction factor as follows:

$F(f^i) = t^i / f^i$

$F(y)$ for $f^i < y < f^{i+1}$ is linearly interpolated between $F(f^i)$ and $F(f^{i+1})$.

Since KF is an adaptive method, f^i is also updated each time the observation y_τ corresponding to the estimates of KF $y_{\tau/\tau-1}$ is available. The update procedure is as follows:

$$f^i_{\tau+1} = \begin{cases} f^i_\tau(1+\alpha) & \text{if } \; y_\tau < t^i \; \text{ and } \; y_{\tau/\tau-1} > f^i \\ f^i_\tau(1-\alpha) & \text{if } \; y_\tau > t^i \; \text{ and } \; y_{\tau/\tau-1} < f^i \\ f^i_\tau & \text{otherwise} \end{cases}$$

where α is an empirical parameter to determine the adaptation speed. This frequency bias correction is applied to the guidance for wind and precipitation amount.

(c) An example of the guidance by Kalman Filter (3-hour precipitation amount)

In this guidance, the predictand is the observed 3-hour accumulated precipitation amount averaged within a 20km x 20km square, and the following nine parameters derived from RSM output are used as predictors.

(i) NW85 : NW-SE component of wind speed at 850hPa
(ii) NE85 : NE-SW component of wind speed at 850hPa
(iii) SSI : Showalter's stability index
(iv) OGES : Orographic precipitation index
(v) PCWV : Precipitable water contents × wind speed at 850hPa × ascending speed at 850hPa
(vi) QWX : Σ (Specific humidity × ascending speed × relative humidity) between 1000 and 300hPa
(vii) EHQ : Σ (Depth of wet layer × specific humidity) between 1000 and 300hPa
(viii) DXQV : Precipitation index on winter synoptic pattern
(ix) FRR : Precipitation by the model (RSM)

Fig. Ⅲ-1 is an example of precipitation forecasts. The observation (A) shows that there was no precipitation in the area M, where the model (C) predicted precipitation whose maximum was over 5 mm/3h. On the other hand, the guidance (B) predicted much less precipitation than the model, showing better results. Examination of the coefficient values at point P revealed that the coefficient of EHQ was the largest and four times as large as that of FRR.

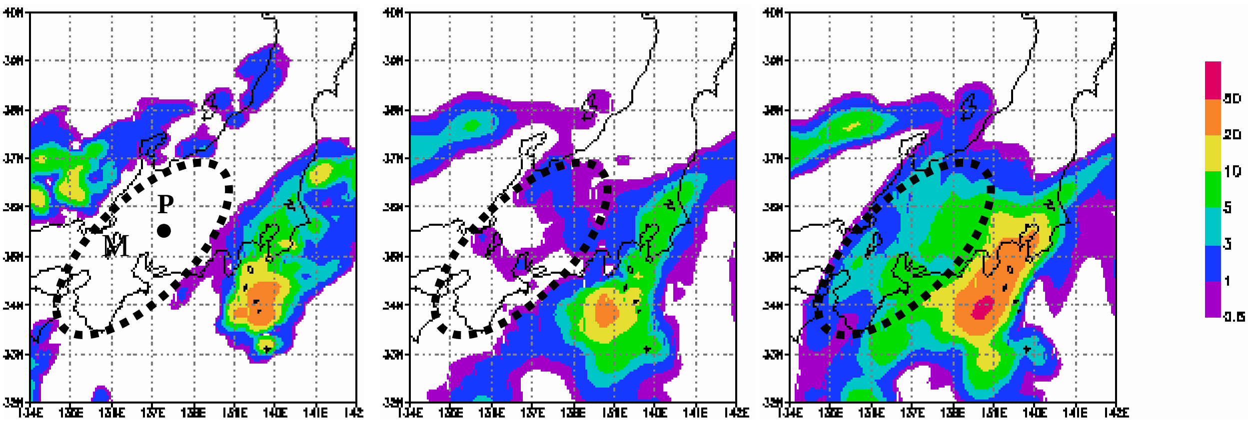

(A) (B) (C)

Fig.Ⅲ-1　Mean precipitation amount over 3 hours. (mm/3hour)
(A) Observation.　(B) Forecast by the guidance.　(C) Forecast by the model (RSM).